Inner-Shell Excitation of Organoiron Compounds by Electron Impact

A. T. Wen, E. Rühl,† and A. P. Hitchcock*

Department of Chemistry, McMaster University, Hamilton, Ontario, Canada L8S 4M1

Received December 9, 1991

Oscillator strengths for the inner-shell excitation (C 1s, O 1s, Fe 2p, and Fe 3p) of eight gas-phase organoiron complexes $Fe(CO)_5$, $Fe_2(CO)_9$, $RFe(CO)_3$ (R = C_4H_6, c-C_6H_8, c-C_8H_8), and $CpFeCpR'$ (R' = H, C_2H_3, C_4H_9) have been derived from electron energy loss spectra recorded under electric dipole scattering conditions. Tentative spectral assignments have been made based upon comparison to the spectra of free ligands and to previous gas-phase studies of related organometallic species. The spectra provide insight into how core excitation spectroscopy reflects the iron–ligand bonding in these complexes. The C 1s, O 1s, and Fe np spectra of related molecules in a series (e.g., carbonyl complexes or ferrocene derivatives) have a similar shape, suggesting similar origins of the spectral features. Small variations through each series have been interpreted in terms of changes in the electronic structure associated with changing substituents. The sensitivity of core spectra to ligand–ligand electronic interaction has been assessed through comparisons to spectral simulations based on the sums of experimental spectra of free ligands and single-ligand complexes. Spectral simulations based on extended Hückel (EHMO) calculations have also been carried out for C 1s and Fe 2p excitation in $Fe(CO)_5$ and $Fe_2(CO)_9$. The Fe 2p spectra are surprisingly sensitive to the type of ligands present in the complexes.

I. Introduction

Organometallic complexes have been receiving considerable attention in both theoretical and experimental chemistry since the discovery of ferrocene. This is chiefly due to the many applications of these compounds in areas such as synthesis, homogeneous catalysis, cluster and solid-state chemistry, chemical vapor deposition of metallic thin films, etc. Molecular spectroscopies have played a pivotal role in organometallic chemistry by addressing problems associated with electronic structure, bonding schemes, molecular formation, and the chemistry of the complexes. Inner-shell excitation by electron energy loss (ISEELS)[1] and X-ray absorption (NEXAFS)[2] spectroscopy has been extended recently to gas-phase organometallic complexes.[3-7] Because of the spatially localized character of core excitation, spectra recorded at several different core edges can be used to map out the unoccupied molecular orbitals (MOs) as they contribute to the various inner-shell electronic excited states of a molecule. Extended Hückel (EHMO) calculations within the equivalent ionic core virtual orbital model[8] (EICVOM) have proven helpful in interpreting ISEELS spectra of organometallic compounds.

The present work is a systematic extension of these studies to organoiron complexes. The spectra of several series of related organoiron complexes have been recorded to investigate the sensitivity of core excitation spectroscopy to the electronic structure, particularly with regard to metal–ligand bonding and ligand–ligand interactions. The spectra of $Fe(CO)_5$ and $Fe_2(CO)_9$ are compared in order to study the sensitivity of core spectra to the weak metal–metal bond predicted by the 18-electron rule. Three iron tricarbonyl complexes with butadiene (C_4H_6), 1,3-cyclohexadiene (c-C_6H_8), and cyclooctatetraene (c-C_8H_8) ligands are used to explore ligand–ligand interaction in mixed ligand complexes. Ferrocene ($FeCp_2$, Cp = η^5-C_5H_5) and two monosubstituted ferrocenes with a vinyl ($CpFeCpCHCH_2$) or a butyl ($CpFeCpC_4H_9$) substituent on one of the Cp rings were used to test the sensitivity of core excitation spectra to more remote perturbations of the electronic structure. ISEELS spectra at the C 1s, O 1s, Fe 2p, and Fe 3p edges of the gas-phase complexes have been recorded using scattering conditions dominated by electric dipole transitions. All spectra, except those at the Fe 3p edge, have been converted to optical oscillator strengths to study trends in the transition probabilities through the molecular series. EHMO calculations have been used to help assign the spectra of the two carbonyl complexes. The C 1s and O 1s spectra of $Fe(CO)_5$ have been presented briefly,[4] while the C 1s spectrum of ferrocene[7] has been discussed in considerable detail previously. All other spectra are being reported for the first time, to our knowledge.

II. Experimental Section

The gas-phase ISEELS spectrometer employed in this work was operated with a high-energy incident electron beam (2.5 keV plus the energy loss) and small scattering angle (<2°), with 0.6-eV FWHM overall resolution. Its basic principles and operating procedures have been described elsewhere.[1] The organoiron complexes were obtained from commercial sources (Strem Chemical Co. and Aldrich). They were used without purification. In some cases, the initial spectra contained contributions from volatile impurities, which disappeared with time through preferential evaporation. In such cases, only spectra acquired after a stable spectral shape was attained were used for further analysis. Where necessary, sample transfers were performed under an inert atmosphere. In a few cases, the solid samples were placed directly inside the vacuum chamber, at a site very close to the incident electron beam, in order to have adequate vapor pressure in the scattering region of the spectrometer. In some cases, the chamber was heated slightly to further increase the signal. In such cases, care was taken to monitor for possible decomposition of the complexes. This was readily detectable in the carbonyl complexes by the appearance of the sharp Rydberg structure of CO around 294 eV. Frequently it was found that decomposition did occur,

†Permanent address: Institut für Physikalische Chemie, Freie Universität Berlin, Takustr. 3, D1000 Berlin 33, Germany.

(1) Hitchcock, A. P. *Phys. Scr.* **1990**, *T31*, 159. Hitchcock, A. P. *Proceedings of Escola Latino-Americana* de *Fisica*; World Scientific Publishing: Singapore, 1991.
(2) Stöhr, J. *NEXAFS Spectroscopy*; Springer: Berlin, 1992.
(3) Rühl, E.; Hitchcock, A. P. *J. Am. Chem. Soc.* **1989**, *111*, 2614.
(4) Hitchcock, A. P.; Wen, A. T.; Rühl, E. *J. Electron Spectrosc.* **1990**, *51*, 653.
(5) Sondericker, D.; Fu, Z.; Bradley, J.; Eberhardt, W. *J. Chem. Phys.* **1990**, *92*, 2203.
(6) Cooper, G.; Sze, K. H.; Brion, C. E. *J. Am. Chem. Soc.* **1989**, *111*, 5051. Cooper, G.; Sze, K. H.; Brion, C. E. *J. Am. Chem. Soc.* **1990**, *112*, 4121.
(7) Rühl, E.; Hitchcock, A. P. *J. Am. Chem. Soc.* **1989**, *111*, 5069.
(8) Schwarz, W. H. E. *Chem. Phys.* **1975**, *11*, 217.
(9) Reference deleted on revision.

0276-7333/92/2311-2559$03.00/0

Table I. Energies (E, eV), Term Values (T, eV), and Proposed Assignments for Features in the C 1s Spectra of CO, $Fe(CO)_5$, and $Fe_2(CO)_9$

CO		$Fe(CO)_5$			$Fe_2(CO)_9$			
E	T^a	no.	E (±0.1)	T	no.	E (±0.1)	T	assignment (final orbital)
287.40	8.7	1	287.80[b]	5.7	1	287.66[b]	5.7	π^*(C=O)
		2 sh	289.3	4.2	2 sh	289.2	4.2	$\pi^*_{delocal}$
		3	290.5	3.0	3	290.6	2.8	$\pi^*_{delocal}$
		4 sh	291.3	2.2	4 sh	291.2	2.2	$\pi^*_{delocal}$
293.3	2.8	5	292.6	0.9	5	292.3	1.1	Rydberg
296.1			293.5			293.4		IP[c]
300.8	-4.7	6	296.2 (4)	-2.7	6	295.6 (4)	-2.2	2e (1s → π^*; 3d → π^*)
304.0	-7.9	7	303.2 (8)	-9.7	7	303.4 (8)	-10	σ^*(C=O)

[a] T = IP − E. [b] Calibration relative to CO_2 (C 1s → π^*: 290.74 eV): ΔE = −2.94 (3) and −3.08 (2) eV for $Fe(CO)_5$ and $Fe_2(CO)_9$, respectively. [c] IPs from XPS.[21] The metal carbonyls have large shake-up. This is the energy of the main XPS line.

but only after several days. We interpret this as indicating that the decomposition was catalyzed by complex fragments or elemental iron produced in the decomposition. The spectra presented here as those recorded before any decomposition had become apparent. Absolute oscillator strengths were obtained by a conversion procedure described elsewhere.[10]

III. EHMO Calculations

Calculations and qualitative descriptions of the MO structure of the ground states of $Fe(CO)_5$,[11] $Fe_2(CO)_9$,[12] $FeCp_2$,[13] and $C_4H_6Fe(CO)_3$[14] have been presented in the literature. These articles give valuable insight into the general characteristics of bonding mechanisms and, in some cases, information about the low-lying unoccupied MOs. Additional semiempirical calculations have been used in this work to obtain a more complete picture of the unoccupied MOs as sampled by core excitation. In some cases, there are large changes in the virtual orbital character between the ground and core excited states because of relaxation of the valence electron distribution in the presence of a localized core hole. EHMO calculations, carried out in the equivalent ionic core virtual orbital model,[8] have been found to account for the relaxation induced by the core hole and to give a satisfactory simulation of the core excitation spectra of many organometallics.[7,15,16] EHMO calculations of the C 1s and Fe 2p spectra of $Fe(CO)_5$ and $Fe_2(CO)_9$ are reported in this work. EHMO results for C 1s excitation of ferrocene have been reported earlier.[7] The molecular geometries used in the calculation were taken from the literature ($Fe(CO)_5$,[17] $Fe_2(CO)_9$[18]). An idealized D_{3h} molecular geometry was adopted for both complexes for simplicity as well as convenience. This seems appropriate since the gas-phase structure of $Fe_2(CO)_9$ is not precisely known. Previous EHMO studies of the metal 2p spectra of Co complexes[15] have indicated a rather strong sensitivity to geometry. The energies and exponents for the Fe atomic orbitals were taken from the same literature source[18] as in our previous studies. As discussed earlier,[15] the results are somewhat sensitive to the choice of Hückel parameters. The same parameters have been used in all calculations in order to have the most meaningful trends through series.

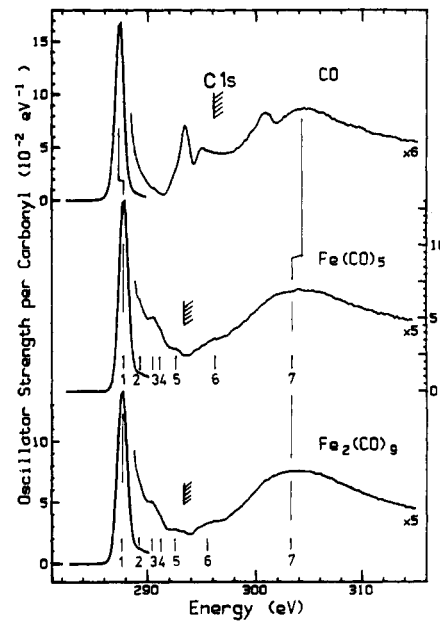

Figure 1. Oscillator strengths for C 1s excitation of CO, $Fe(CO)_5$, and $Fe_2(CO)_9$ derived from inner-shell electron energy loss spectra (ISEELS) measured under conditions of 2.5-keV final electron energy, 2° scattering angle, and 0.6-eV FWHM resolution. The hatched lines indicate the location of the C 1s ionization potentials as determined by XPS.[21]

The EHMO results were used to generate spectral simulations, as described previously.[15] As an example, the EHMO simulation of C 1s excitation at the axial carbonyl of $Fe(CO)_5$ is the sum of Gaussian lines with relative positions given by the virtual orbital energies, a width of 1.0 eV fwhm and intensities given by $\sum c^2(N2p)$ where $c(N2p)$ is the LCAO coefficient, the contribution of the N 2p AO to the virtual MO in the molecule where a N atom replaces one of the axial carbonyl carbon atoms to account for the core hole within the equivalent core approximation. A similar calculation and spectral simulation was carried out for C 1s excitation of an equatorial carbonyl. The EHMO simulation of the complete C 1s spectrum of $Fe(CO)_5$ is a 2:3 weighted sum of these component spectra. The energy scale of this simulation should approximate the experimental term values. In fact, EHMO energies are typically too low by about 4 eV. More suggestive comparisons have been made by aligning the most prominent feature of the EHMO simulation with that of the main feature in the experimental spectrum.

IV. Results and Discussion

1. C 1s Spectra. A. Iron Carbonyl Complexes. The C 1s spectra of $Fe(CO)_5$ and $Fe_2(CO)_9$ are compared to that

(10) Mclaren, R.; Clark, S. A. C.; Ishii, I.; Hitchcock, A. P. *Phys. Rev. A* **1987**, *36*, 1683.
(11) Guenzburger, D.; Saitovitch, E. M. B.; DePaoli, M. A.; Manela, H. *J. Chem. Phys.* **1984**, *80*, 735. Olthoff, J. K.; Moore, J. H.; Tossell, J. A.; Giordan; J. C.; Baerends, E. J. *J. Chem. Phys.* **1987**, *87*, 7001.
(12) Heijiser, W.; Baerends, E. J.; Ros, P. *Faraday Symp. Chem. Soc.* **1980**, *14*, 211 and references therein.
(13) Haaland, A. *Acc. Chem. Res.* **1979**, *12*, 415 and references therein.
(14) Albright, T. A.; Burdett, J. K.; Whangbo, M. H. *Orbital Interactions in Chemistry*; John Wiley & Sons: New York, 1985; p 368. Elian, M.; Hoffmann, R. *Inorg. Chem.* **1975**, *14*, 1058.
(15) Rühl, E.; Wen, A. T.; Hitchcock, A. P. *J. Electron Spectrosc.* **1991**, *57*, 137.
(16) Hitchcock, A. P.; Wen, A. T.; Rühl, E. *Chem. Phys.* **1990**, *147*, 51.
(17) Evens, R. V. G.; Lister, M. W. *Trans. Faraday Soc.* **1939**, *35*, 681.
(18) Cotton, F. A. *Prog. Inorg. Chem.* **1976**, *21*, 1.
(19) Albright, T. A.; Hoffmann, P.; Hoffmann, R. *J. Am. Chem. Soc.* **1977**, *99*, 7546.

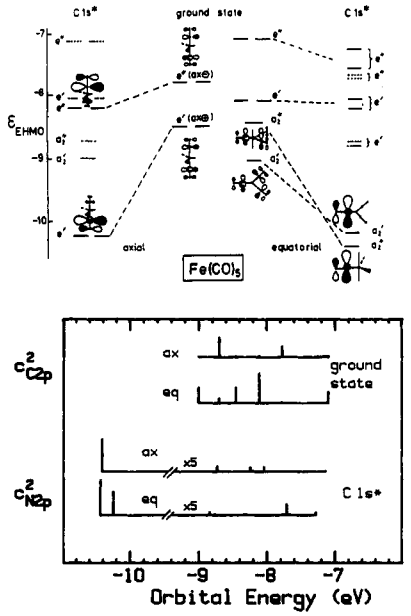

Figure 2. EHMO results for the π^* orbitals of $Fe(CO)_5$ in both the ground state and in the presence of C 1s core holes. The upper portion sketches the orbital energies and selected orbital shapes. The lower portion presents the spectra on an EHMO orbital energy scale with intensities given by the square of the C 2p (ground state) or N 2p (C 1s excitation) LCAO coefficients in the π^* orbitals. Note the carbon atom considered for the spectra derived from the ground-state calculation is the same as that which is replaced by the $(Z + 1)$ N atom in the C 1s excited-state calculation.

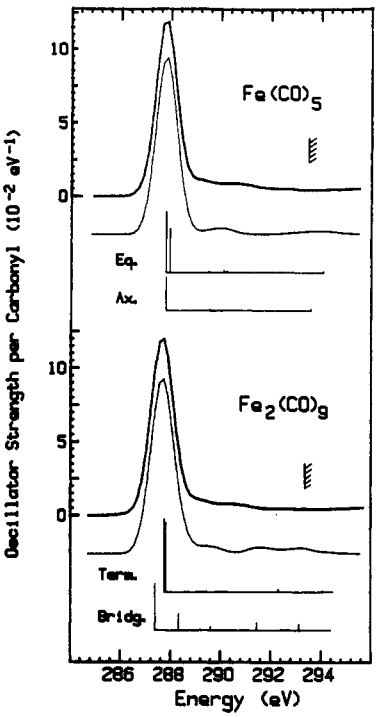

Figure 3. Simulated spectra (light solid line) derived from EHMO calculations compared to the experimental spectra (dark solid line) of $Fe(CO)_5$ and $Fe_2(CO)_9$. The simulations are the weighted sum of components associated with C 1s excitation at the two different types of C atoms in each species. The individual lines of the simulation are Gaussians of 1.0-eV FWHM with a relative position given by the virtual orbital energy and an intensity given by $\sum c^2(N2p)$. The absolute energy scale of the weighted sum was set by aligning the main peak in the simulation to the main C 1s $\rightarrow \pi^*$ peak in the experimental spectrum. The intensity of the EHMO-simulated spectrum was established by matching the main π^* peak area to the experimental value. The vertical lines under the simulated spectra indicate the positions and relative intensities of the lines of the component spectra.

of free CO in Figure 1. Energies, term values, and proposed assignments of the spectral features are listed in Table I. The spectra of the two metal carbonyl species are quite similar. Each is dominated by an intense, low-energy peak corresponding to C 1s $\rightarrow \pi^*$(C=O) excitation localized on a single carbonyl ligand. Several weak features are apparent between 289 and 292 eV, just above the main π^*(CO) resonance. These are assigned to C 1s $\rightarrow \pi^*_{delocal}$ transitions, which may be thought of as a type of charge transfer since the majority of the density of these orbitals is on carbonyl ligands other than that containing the C 1s hole.

The distinction that is being made between π^*_{local} and $\pi^*_{delocal}$ is well-illustrated by a comparison of the EHMO results for ground-state and C 1s excited $Fe(CO)_5$ (Figure 2). In the ground state, the 10 π^*(CO) orbitals may be divided into axial and equatorial sets, in each case delocalized over several carbonyl ligands. If the C 1s spectrum reflected the π^* orbitals of the ground state, the C 1s $\rightarrow$ π^* region of the spectrum would consist of six rather intense transitions distributed over 2 eV (upper part of the lower panel of Figure 2). The resulting spectrum would exhibit obvious shoulders at our experimental resolution (0.6 eV) and clearly separated peaks at state-of-the-are resolution (45 meV). However, the carbon 1s core hole modifies the virtual orbitals substantially. The lowest energy virtual orbital becomes strongly localized on the C 1s excited carbonyl and is stabilized by more than 1 eV relative to the ground state. At the same time, the higher energy π^* orbitals are either unchanged or are "antilocalized" on carbonyl ligands without the C 1s core hole. The energies of the antilocalized MOs are unchanged or only slightly stabilized relative to the ground state. Thus, when the effect of the core hole is taken into account, EHMO predicts the main C 1s $\rightarrow \pi^*$ intensity in $Fe(CO)_5$ to be associated with three components, a doubly degenerate π^*_{local}(ax) and two orthogonal π^*_{local}(eq) resonances, separated by 0.2 eV. At higher energy, EHMO predicts weak features corresponding to small N 2p contributions to the antilocalized or unmodified π^* orbitals. It is the latter that are denoted C 1s $\rightarrow \pi^*_{delocal}$ transitions.

As shown in Figure 3, the spectral simulations derived from EHMO calculations agree well with the experimental C 1s spectra of $Fe(CO)_5$ and $Fe_2(CO)_9$. The simulations are the weighted sum of two components: $[2(C_{axial}) + 3(C_{equatorial})]$ in $Fe(CO)_5$ and $[3(C_{bridging}) + 6(C_{terminal})]$ in $Fe_2(CO)_9$. These components each consist of several lines as indicated in Figure 3. EHMO simulates the discrete portion of the experimental C 1s spectra of both species reasonably well, reproducing both the extraordinary concentration of the oscillator strength in the lowest energy π^*_{local} feature as well as the weakness and some aspects of the energy distribution of the C 1s $\rightarrow \pi^*_{delocal}$ transitions. However, the EHMO calculations suggest there should be additional bands at 291.5 and 293 eV in $Fe_2(CO)_9$ which are not evident in the experimental spectrum. These features could be present but are not observed as distinct features in the experimental spectra on account of overlap with Rydberg transitions which the minimal basis set EHMO treatment cannot predict.

The oscillator strengths for 1s $\rightarrow \pi^*$(C=O) features (and the π^*(C=C) resonances, in the other complexes) have been derived by peak area measurements using Gaussian curve fits. These results are summarized in Table II. The main π^* resonance of the carbonyl complex is less intense than that of the π^*(CO) resonance of CO. However, on a per carbonyl basis, the *sum* of the oscillator strengths

Table II. Integrated Intensities (f, $\times 10^{-2}$) of 1s → π^* Transitions in Organoiron Complexes

species	C 1s π^*(CO)[a] π^*_{local}	C 1s π^*(CO)[a] $\sum\pi^*_{delocal}$	C 1s π^*(CO)[a] $\sum\pi^*$(C=O)	C 1s π^*(C=C)[a]	O 1s π^*(C=O)[a] π^*_{local}	O 1s π^*(C=O)[a] $\pi^*_{delocal}$	O 1s π^*(C=O)[a] $\sum\pi^*$(C=O)
CO	18.0		18.0		7.51		7.51
$Fe(CO)_5$	14.9	2.8	17.7		7.20	0.58	7.78
$Fe_2(CO)_9$	16.0	2.3	18.3		6.25	1.70	7.95
C_4H_6				12.4			
$C_4H_6Fe(CO)_3$	13.6	2.6	16.2	12.2[b]	6.41	0.49	6.90
C_6H_8				13.9			
$C_6H_8Fe(CO)_3$	(17.3)[c]	(3.1)[c]	(20.4)[c]	12.2	5.83	0.89	6.72
C_8H_8				31.2[d]			
$C_8H_8Fe(CO)_3$	(19.7)[c]	(4.3)[c]	(24.0)[c]	17.9	5.93	1.02	6.95

[a] The oscillator strengths for π^*(C=O) are given per carbonyl for ease of comparison. The values for π^*(C=C) are not normalized per C=C bond. [b] This is the area of all structures below the main π^*(C=O) line. [c] These f values are believed to be too high because of contributions from underlying C 1s → π^*(C=C) transitions. [d] This value includes the π^*(C=C) signal which most likely underlies the π^*(C=O) feature in the $C_8H_8Fe(CO)_3$ complex.

Table III. Energies (E, eV), Term Values (T, eV), and Proposed Assignments for Features in the C 1s Spectra of $C_4H_6Fe(CO)_3$, c-$C_6H_8Fe(CO)_3$, and c-$C_8H_8Fe(CO)_3$

$C_4H_6Fe(CO)_3$ no.	E	T CH	T CO	c-$C_6H_8Fe(CO)_3$ no.	E	T CH	T CO	c-$C_8H_8Fe(CO)_3$ no.	E	T CH	T CO	assignment (final orbital) CH	assignment (final orbital) CO
								1	284.2	6.2		π^*(C=C) (non-Fe)	
1	284.9	5.9		1	285.1	5.4		2 sh	284.8	5.6		π^*(C=C)	
2	285.5	5.3		2	285.8	4.7		3 sh	285.5	4.9		Fe 3d	
3	287.77[a]		5.43	3	287.74[a]		5.26	4	287.67[a]		5.13		π^*(C=O)
4	289.7		3.0	4	289.8		3.2	5	289.4		3.4		$\pi^*_{delocal}$
	290.8[b]				290.5[c]				290.4[c]			IP[b](C—H)	
5	292.4	−1.6		5	292.3	−1.8		6	293.3	−2.9		σ^*(C—C)	
	293.2[b]				293.0[c]				292.8[c]				IP(C=O)
6 br	298 (1)	−7.2		6	299 (1)	−8.5		7	298 (1)	−7.6		σ^*(C=C)	
7	301.2 (8)		−8	7	301.2 (8)		−8	8	301 (1)		−8		σ^*(C=O)

[a] Calibration relative to CO_2: ΔE = −2.97 (4), −3.00 (3), and −3.07 (3) eV for $C_4H_6Fe(CO)_3$, c-$C_6H_8Fe(CO)_3$, and c-$C_8H_8Fe(CO)_3$, respectively. [b] IPs from XPS.[21] [c] IPs estimated from those of related species ($C_7H_8Fe(CO)_3$).[21]

of the $\pi^*(CO)_{local}$ and $\pi^*(CO)_{delocal}$ resonances is in rather good agreement with the π^* oscillator strength for CO. This observation supports our $\pi^*(CO)_{delocal}$ assignment since this observation is consistent with a simple redistribution of C 2p contributions to the π^* orbitals.

Relative to CO, Rydberg structures and double excitations are much less prominent in the metal carbonyls. Their intensities seem to be substantially diminished, either because of extensive mixing with valence orbitals (of which there is a higher density) or because large-R Rydberg orbitals are excluded from the C 1s core region by virtue of the large size of the molecule.

One motivation of the EHMO study was to investigate the possible occurrence and energy position of a postulated C 1s → σ^*(Fe–Fe) transition in $Fe_2(CO)_9$. EHMO predicts an orbital of unambiguous σ^*(Fe–Fe) character at ϵ = −7.9 eV for excitation at the bridging carbonyl and ϵ = −8.7 eV for excitation at the terminal carbonyl. Energetically C 1s excitation to these orbitals would lie at 289 or 290 eV, but EHMO predicts zero intensity since there is no N 2p contribution to these orbitals; i.e., there should not be any signal arising from C 1s → σ^*(Fe–Fe) transitions. This agrees with experiment and our previous studies of $Mn_2(CO)_{10}$[3] and $Co_2(CO)_8$[15] where evidence for C 1s → σ^*(M–M) features was sought but also not found. Basically, if there is a well-localized σ^*(M–M) virtual orbital, it is not likely to be significant in the C 1s spectrum because of poor spatial overlap with the C 1s core orbital.

The σ^*(C=O) shape resonances in the C 1s spectra of the metal carbonyls occur about 1 eV lower in energy than that in free CO, as found in other transition-metal carbonyls.[3-6] This is consistent with the increase in C–O bond length and the weakening of the CO bond, as predicted by the dπ–pπ back-donation model for bonding of CO to metals.[20] The σ^* shape resonance is considerably broader than that in free CO. This could be related to the existence of numerous closely-spaced final states in this region. Alternatively, the σ^* resonances of metal carbonyls could decay into the direct C 1s ionization continuum more rapidly than in CO. The photoelectron at the metal carbonyl σ^* peak has a greater kinetic energy than in CO since the C 1s IP of the metal carbonyls is about 2 eV below that of CO.[21] This should lead to an increase of 2 eV in the resonance width according to a published correlation between photoelectron energy and resonance width.[22] This is in reasonable agreement with the observed increase in resonance width.

B. Iron Tricarbonyl Complexes with Unsaturated Hydrocarbon Ligands. The C 1s spectra of three organoiron complexes ($RFe(CO)_3$, R = butadiene, cyclohexadiene, and cyclooctatetraene) are presented in Figure 4. The energies, term values, and tentative assignments for the spectral features are listed in Table III. The spectra of these three complexes are similar, indicating that the most intense features involve excitations to virtual orbitals associated with the $Fe(CO)_3$ fragment which is common to all three species. The sharp, intense peaks at 287.7 eV are attributed to the main C 1s → $\pi^*(C{=}O)_{local}$ transition. These occur at essentially the same energy as in the pure carbonyl complexes. The weak feature observed around 289.7 eV in each species is attributed to C 1s → $\pi^*_{delocal}$ transitions (see Figure 5 for an expanded plot

(20) Dewar, M. J. S. *Bull. Soc. Chim. Fr.* **1951**, C17. Chatt, J.; Duncanson, L. A. *J. Chem. Soc.* **1953**, 2939.
(21) Jolly, W. L.; Bomben, K. D.; Eyermann, C. J. *At. Data Nucl. Data Tables* **1984**, *31*, 433.
(22) Connerade, J. P. *J. Phys. B* **1984**, *17*, L165.

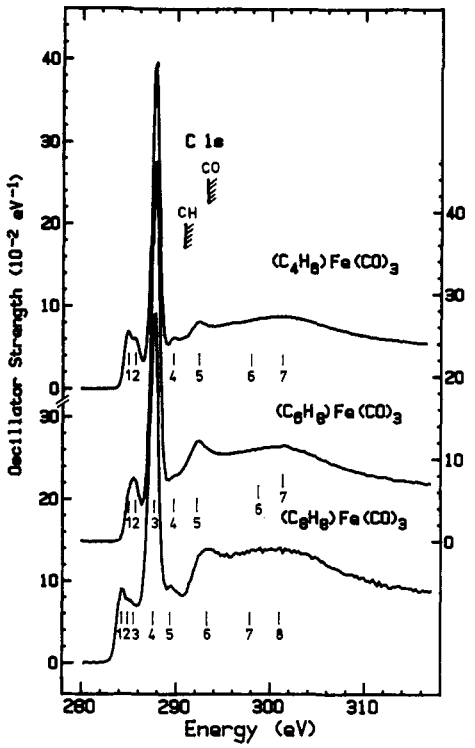

Figure 4. Oscillator strengths for C 1s excitation of $(C_4H_6)Fe(CO)_3$, $(c\text{-}C_6H_8)Fe(CO)_3$, and $(c\text{-}C_8H_8)Fe(CO)_3$ derived from ISEELS spectra recorded under the conditions as described in Figure 1. Hatched lines indicate estimated C 1s IPs.

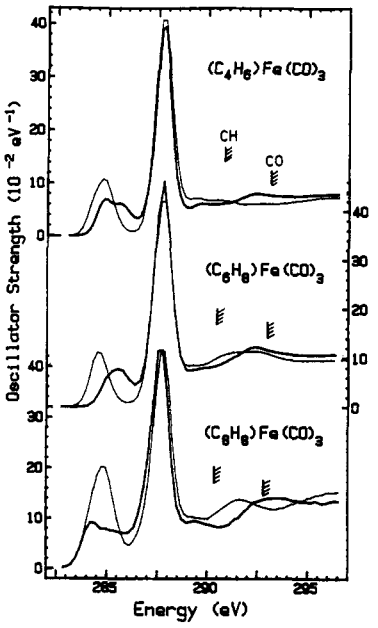

Figure 5. Comparison of the experimental C 1s spectra (dark line) of $RFe(CO)_3$ (R = butadiene, 1,3-cyclohexene, and cyclooctatetraene) and simulations generated by summing the C 1s spectrum of R with 0.6 times that of $Fe(CO)_5$ (light line).

of this spectral region). In the continuum, there are two major σ^* shape resonances for each complex. The first resonance at 292 eV is assigned to C 1s excitations to a σ^* MO associated mainly with the C–C single bonds of the polyenes. The second broad peak, that between 298 and 304 eV, likely contains contributions from both σ^*(C=C) and σ^*(C=O) resonances. Based on the bond length correlation and the spectra of related species, these are expected around 299 and 303 eV, respectively.

According to literature MO schemes[14] of $RFe(CO)_3$ complexes where R is a diene, the LUMO is concentrated mainly on the diene portion of the complex, while the next-to-LUMO is concentrated at the Fe metal. Consequently, the lowest energy band in the C 1s spectrum of each complex (e.g., that at 284.9 eV in $C_4H_6Fe(CO)_3$) is assigned to C 1s $\rightarrow \pi^*$(C=C) transitions. For the $c\text{-}C_6H_8$ complex, this feature only appears as a weak shoulder on the low-energy side of the first peak and is not as well-resolved as in the spectra of the C_4H_6 and $c\text{-}C_8H_8$ derivatives. Above the feature associated with the LUMO, there is another feature at 285.5 eV. This is assigned to C 1s excitations to the next-to-LUMO, an orbital that is based largely on the Fe atom. The C 1s spectrum of $CpCo(CO)_2$[15] greatly resembles that of $c\text{-}C_6H_8Fe(CO)_3$ in this low-energy region. It seems that ligands having a 5- or 6-membered ring structure, such as $C_5H_5^-$ and $c\text{-}C_6H_8$, mix effectively with the metal 3d orbitals of the $M(CO)_n$ fragment. This results in spectra which exhibit unresolved, broad bandlike peaks formed by the overlap of several transitions.

The η^4 bonding between the metal and the unsaturated hydrocarbon ligands (R) is through electron donation from a diene to the $Fe(CO)_3$ fragment, which is a good acceptor by virtue of its three CO ligands. Thus, as in $CpCo(CO)_2$,[15] a net charge transfer from the dienes to the carbonyls is expected in all three of these complexes. Can we see spectral modifications reflecting this charge transfer, similar to those which were identified in the C 1s spectrum of $CpCo(CO_2)$? The effects of ligand–ligand interactions in mixed ligand complexes should be best identified by comparison of the experimental spectrum with that of a weighted sum of the C 1s spectra of FeR_2 and $Fe(CO)_5$. However, although the spectra of the free hydrocarbon ligands are available, the FeR_2 complexes which would be required to characterize the Fe–R bonding interaction are not known. Instead we have prepared simulations which are the sum of the C 1s spectrum of the free diene ligand[4,23,24] with 0.6 times that of $Fe(CO)_5$. Figure 5 compares the discrete region of the experimental C 1s spectra with these experimentally derived spectral simulations. Such simulations should give insight into the modifications of the virtual orbitals of the R group caused by metal–ligand interaction. It should also provide some information concerning the possible effects of ligand–ligand interaction on the carbonyl orbitals.

The simulation of the $C_4H_6Fe(CO)_3$ complex supports assignment of the lowest energy peak to C 1s $\rightarrow \pi^*$(C=C) transitions on the diene ligand, but it does not predict the 285.6-eV feature that we have attributed to excitations to Fe-3d-dominated MOs. This is understandable since a simulation consisting of the spectrum of free ligand R and $Fe(CO)_5$ cannot be expected to predict spectral features associated with Fe–R antibonding levels. Thus, one can infer from the comparison that the C 1s spectrum of the hypothetical species $Fe(C_4H_6)_2$ should contain a feature around 286 eV which would be a result of the C_4H_6–Fe interaction. This feature would be analogous to the C 1s $\rightarrow 4e_{1g}$ ($3d_{xz,yz}$) transition in the metallocenes,[7] and thus, we label such transitions "$4e_{1g}$" to emphasize the analogy with ferrocene. In all three species, the diene–metal interaction causes a marked suppression of the C 1s $\rightarrow \pi^*$ intensity on the diene and introduction of one or two additional levels at slightly higher energy, apparently of mixed π^*(C=C) and Fe 3d character. The discrepancy between simulation and experiment is greatest for the

(23) Hitchcock, A. P.; Beaulieu, S.; Steel, T.; Stöhr, J.; Sette, F. *J. Chem. Phys.* **1984**, *80*, 3927.
(24) Hitchcock, A. P.; Newbury, D. C.; Ishii, I.; Stöhr, J.; Horsley, J. A.; Redwing, R. D.; Johnson, A. L.; Sette, F. *J. Chem. Phys.* **1986**, *85*, 4849.

Table IV. Energies (E, eV), Term Values (T, eV), and Proposed Assignments for Features in the C 1s Spectra of $CpFeCpCH{=}CH_2$, CpFeCpH, and $CpFeCpC_4H_9$

$CpFeCpC_2H_3$				$FeCp_2$			$CpFeCpC_4H_9$			assignment (final orbital)	
no.	E	T_{Cp}	T_R	no.	E	T	no.	E	T	Cp	R
1 sh	284.4		6.4								$\pi^*(CH{=}CH_2)$
2	285.6	4.5		1	285.7	4.3	1	285.6	4.4	"$4e_{1g}$"(Fe 3d)	
3	287.14[a]	2.91		2	287.21[a]	2.82	2	287.18[a]	2.82	π^*(Cp)	
4	289.1	0.9	1.7	3	289.0	1.0	3	289.0	1.0	σ^*(CH)	σ^*(CH)
	290.0[c]				290.03[b]			290.0[c]		IP(Cp)	
	290.8[c]										IP(C_2H_4)
5	292.3	−2.3		4	292.2	−2.2	4	292.4	−2.4	σ_1^*(C═C)	σ^*(C—C)
6	298 (1)	−8		5	298	−8	5	298.0 (5)	−8	σ_2^*(C═C)	σ^*(C═C)
7	302 (1)	−11					6	301.4 (8)	−11.4	shake-up	shake-up

[a] Calibration relative to CO_2: ΔE = −3.60 (4), −3.53 (2), and −3.56 (3) eV for $CpFeCpCH{=}CH_2$, $FeCp_2$, and $CpFeCpC_4H_9$, respectively. [b] IPs from XPS.[21] [c] IPs assumed to be the same as for ferrocene and ethene.

c-C_8H_8 complex, implying a stronger interaction between the c-C_8H_8 and $Fe(CO)_3$ fragments than in the other two species. According to the simulation, the spectrum of c-$C_8H_8Fe(CO)_3$ should be much more intense in the diene π^* region than observed. Cyclooctatetraene (COT) has three low-energy π^* resonances at 284.8, 287.3, and 289.3 eV.[24] Since the η^4-diene bonding involves only two of the four C═C bonds in COT, the π^* orbitals associated with those two bonds should mix more extensively with the Fe 3d orbitals than those associated with the two C═C bonds which are remote from the iron. There is negligible delocalization in COT due to the nonplanar structure. Thus, it is conceivable that part of the π^* density is rather similar to that in free COT, giving rise to the low-energy π^*(C═C) structure at 284.2 eV which is much less intense but otherwise similar to the lowest π^* feature in COT (284.8 eV). The π^*(C═C) MOs at the η^4 bond are extensively modified through mixing with Fe 3d. The latter would then give rise to the features at 284.8 and 285.5 eV, which are similar to those observed in the spectra of the other Fe–diene complexes.

The C 1s → $\pi^*(C{=}O)_{local}$ transition is much more intense than the C 1s → π^*(C═C) transition. *Why*? π^*-(C═C) resonances are intrinsically weaker than π^*(C═O) resonances.[10] This difference is further magnified because Fe 3d orbitals mix better with π^*(C═C) than with π^*-(C═O) MOs owing to more appropriate spatial and energy matches between the metal 3d and the diene π^* orbitals. Strong back-donation of metal 3d density into the empty π^* orbital of the polyene can be thought of as "blocking" the promotion of the C 1s electron into this π^* orbital, thus diminishing the transition probability. Less pictorially, but more correctly, the reduced intensity is associated with changes in the orbital mixing which result in a smaller C 2p contribution to the dπ–pπ orbital. This point is well-illustrated by Figure 5. In each species the experimental feature associated with π^*(C═C) is much weaker than predicted by the simulation.

We expect the $RFe(CO)_3$ spectra to be influenced by charge transfer between the donating diene and the accepting carbonyls. From analogy to $CpCo(CO)_2$,[15] notable effects should include a weaker π^*(CO) resonance and a stronger "$4e_{1g}$" peak, than in the FeR_2 and $Fe(CO)_5$ complex. Although we cannot compare to FeR_2, a comparison of the π^*(CO) intensity of $Fe(CO)_5$ and that of the $RFe(CO)_3$ complexes should be sensitive to the ligand–ligand interaction. The integrated π^*(CO) oscillator strengths (per carbonyl) for all species are summarized in Table II. While the precision of the peak integration is not high because of its sensitivity to details of background subtraction, the results do seem to support the expected charge transfer in $C_4H_6Fe(CO)_3$. The evidence is contradictory in the other two $RFe(CO)_3$ complexes. In these other species, $f(\pi^*_{co})$ is greater than in free CO, presumably because of contributions from underlying C 1s → π^*(C═C) transitions on the C_6H_8 and C_8H_8 ligands.

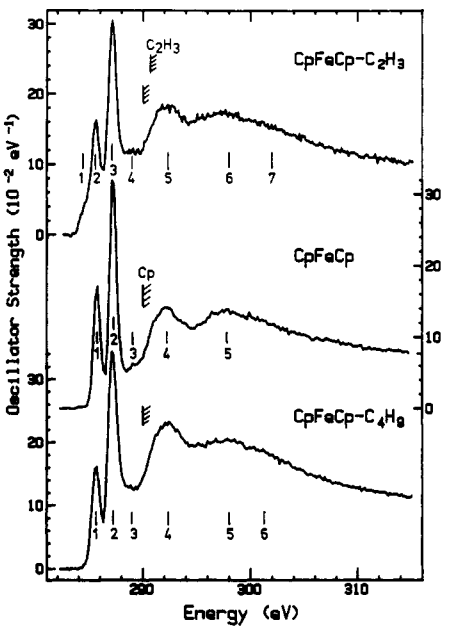

Figure 6. Oscillator strengths for C 1s excitation of $CpFeCpC_2H_3$ (Cp: η-C_5H_5), $FeCp_2$, and $CpFeCpC_4H_9$ derived from ISEELS spectra recorded under the conditions described in Figure 1.

C. Substituted Ferrocenes. The C 1s spectra of $FeCp_2$ and the two ring-substituted ferrocenes are presented in Figure 6. Energies, term values, and proposed assignments are given in Table IV. This comparison shows directly that substituents on the Cp ring have little influence on the basic electronic structure of ferrocene, since the spectra of all three species exhibit the four major spectral features of ferrocene. There is an additional low-energy feature in the spectrum of $CpFeCpC_2H_3$ which is associated with C 1s → π^* transitions at the vinyl substituent. The C 1s excitations at the butyl substituent do not appear to give rise to distinct features, but changes in the relative intensities of the four ferrocene features are consistent with broad underlying bands at the positions expected from the C 1s spectrum of butane.[25] The sharp peak at 285.6 eV is assigned to C 1s → $4e_{1g}$ ($3d_{xz,yz}$) in ferrocene[3] and to a "$4e_{1g}$-like" orbital in the other two species. The main line at 287.2 eV is attributed to C 1s → π^*(Cp) transitions. The intensity between the π^*(Cp) resonance and the ionization potential is attributed to the overlap of C 1s → σ^*(C–H)[25] and Rydberg transitions.

(25) Hitchcock, A. P.; Ishii, I. *J. Electron Spectrosc.* **1987**, *42*, 11.

Table V. Energies (E, eV), Term Values (T, eV), and Proposed Assignments for Features in the O 1s Spectra of CO, $Fe(CO)_5$, $Fe_2(CO)_9$, $C_4H_6Fe(CO)_3$, c-$C_6H_8Fe(CO)_3$, and c-$C_8H_8Fe(CO)_3$

CO		$Fe(CO)_5$			$Fe_2(CO)_9$			$C_4H_6Fe(CO)_3$			$C_6H_8Fe(CO)_3$			$C_8H_8Fe(CO)_3$			assignment (final orbital)
E	T	no.	E	T	no.	E	T	no.	E	T	no.	E	T	no.	E	T	
534.1	8.3	1	533.8[a]	5.7	1	533.9[a]	5.8	1	533.9[a]	5.1	1	533.9[a]	5.2	1	533.7	5.4	π^*(C=O)
					2	536.2	3.5	2	536.0	3.0	2	536.0	3.0	2 sh	535.3	3.8	$\pi^*_{delocal}$
		2	537.2	2.3	3	537.6	2.1							3 sh	536.6	2.4	$\pi^*_{delocal}$
541.0	1.4	3	537.9	1.6													Rydberg
542.4[b]			539.5[b]			539.7[b]			539.0[b]			539.0[c]		539.0[c]			IP
		4	539.8 (4)	−0.3	4	539.5	0.2	3	539.6 (4)	−0.6	3	539.2 (4)	−0.3	4	540.0 (4)	−1.0	cont onset?
551.0 (8)	−8.5	5	549.9 (8)	−10	5	549.5 (8)	−9.8	4	549.8 (8)	−11	4	549.8 (8)	−11	5	550.0 (8)	11	σ^*(C=O)

[a] Calibration relative to CO_2 (O 1s → π^*: 535.4 eV): ΔE = −1.60 (6) and −1.50 (8) eV for $Fe(CO)_5$ and $Fe_2(CO)_9$, respectively. Calibration relative to O_2 (530.8 eV): ΔE = 3.07 (7), 3.10 (7), and 2.90 (8) eV for $C_4H_6Fe(CO)_3$, $C_6H_8Fe(CO)_3$, and $C_8H_8Fe(CO)_3$, respectively. [b] IPs from XPS.[21] [c] Estimated from the O 1s IP of $C_4H_6Fe(CO)_3$.

These features are stronger in the spectra of the two ferrocene drivatives, perhaps because these two complexes contain more C–H bonds.

As discussed previously,[26] there is very strong interaction of σ^* orbitals associated with adjacent C–C bonds in a localized bond orbital description of aromatic ring structures. This produces a large splitting in the energies of σ^*(C–C) orbitals which leads to two prominent continuum resonances in ferrocene. The strong band at 292 eV in the continuum is labeled the σ_1^*(C=C) shape resonance, while the intense, broad band around 298 eV is labeled the σ_2^*(C=C) shape resonance. Both are associated with the Cp ring. For the two ring-substituted ferrocenes, the continuum resonances are more intense than the 286-eV $4e_{1g}$-like excitation, whereas the opposite is the case for ferrocene. Since the intensities of the $4e_{1g}$-like and π^*(Cp) transitions are rather constant in all three species, this implies the change in the relative intensity of discrete and continuum features is associated with more intense continuum features, consistent with additional contributions from σ^* resonances associated with the C–C bonds of the group attached to the Cp ring.

The low-energy shoulder at 284.5 eV in the C 1s spectrum of $CpFeCpC_2H_3$, is assigned to excitations to the π^* level of the vinyl substituent. Spectral simulation supports this assignment. In Figure 7, the experimental spectra of both derivatives are compared to simulations created from the sum of the C 1s spectrum of the ring substituent (ethene[10] and butane[25]) and that of $Fe(Cp)_2$. The simulation suggests that the lowest energy π^*(C=C) feature of $CpFeCpC_2H_3$ should be more intense than observed. This indicates there is significant interaction between the vinyl π^*(C=C), the π^*(Cp), and the Fe 3d orbitals such that the contribution of C 2p orbitals of the vinyl substituent to "π^*(C=C)" is considerably less than in free ethylene. Overall the simulated spectrum of $CpFeCpC_2H_3$, although it does predict all major spectral features, has significant disagreement regarding relative intensities. This is expected since the vinyl substituent interacts with the Fe 3d orbitals through the Cp ring, an effect which this type of simulation cannot be expected to reproduce. The simulated and experimental spectra of $CpFeCpC_4H_9$ are in much better agreement. This may be interpreted in terms of a poor energy and spatial match and thus less mixing between the Fe 3d orbitals and the virtual orbitals of the alkyl group relative to that with the π^*(C=C) orbitals. This observation is consistent with that of Waite and Papadopoulis,[27] who note that a vinyl has a much larger effect than a methyl substituent on the polarizability and valence charge transfer excitations of substituted ferrocenes.

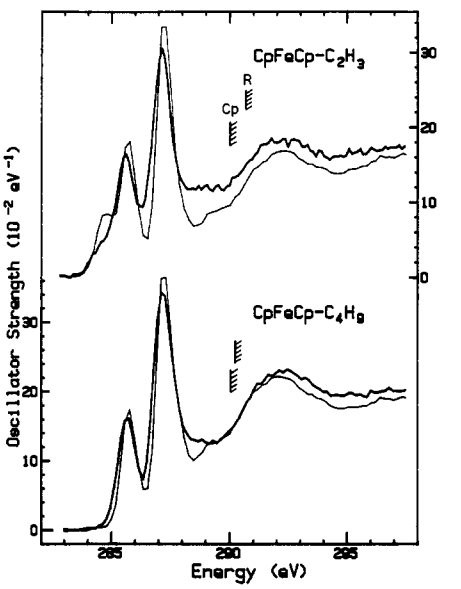

Figure 7. Comparison of the experimental C 1s spectra of CpFeCpR (R = C_2H_3 and C_4H_9) (dark line) and simulations which are the sum of the C 1s spectra of RH (ethene and butane) and $Fe(CP)_2$ (light line).

2. O 1s Spectra. The O 1s spectra of all five oxygen-containing complexes, two iron carbonyl and three mixed ligand, are presented in Figure 8, along with that of CO. The energies, term values, and proposed assignments of the O 1s spectral features are given in Table V. The O 1s spectra of all carbonyl complexes have very similar shapes and energies. As in the O 1s spectrum of CO, the two main features are the intense O 1s → π^*(C=O) transition and the strong, broad σ^*(C=O) shape resonance in the continuum. The π^* resonance occurs at 533.8 ± 1 eV in the complexes. This is about 0.3 eV lower than the energy of the O 1s → π^* resonance in CO. The interpretation of the energy shift of the π^*(C=O) excitation has been discussed in detail previously.[3] The σ^* resonances occur around 550 eV, about 1 eV below the corresponding σ^* resonance in CO. As discussed for the corresponding C 1s → σ^*(CO) feature (section IV.1.A), the decrease in the energy of the σ^*(C=O) shape resonance is believed to be associated with weakening of the C=O bond by virtue of back-donation from Fe. The back-donation also reduces the oscillator strength of the O 1s → π^*(C=O) transition[4] by almost 20% (see Table II).

In addition to the intense O 1s → π^*(C=O) and σ^*(C=O) resonances, weak O 1s → $\pi^*_{delocal}$ transitions can be detected around 536–537 eV. These are most visible in $Fe_2(CO)_9$ and c-$C_8H_8Fe(CO)_3$, but a careful examination of the data reveals that similar structures occur in the O 1s spectra of all of these complexes. An ill-defined structure attributable to Rydberg transitions occurs around

(26) Hitchcock, A. P.; Stöhr, J. *J. Chem. Phys.* **1984**, *87*, 3253.
(27) Waite, J.; Papadopoulis, M. G. *J. Phys. Chem.* **1991**, *95*, 5426.

Table VI. Energies (E, ±0.2 eV), Term Values (T, eV), and Proposed Assignments for Features in the Fe 2p Spectra of $Fe(CO)_5$, $Fe_2(CO)_9$, $C_4H_6Fe(CO)_3$, c-$C_6H_8Fe(CO)_3$, and c-$C_8H_8Fe(CO)_3$

$Fe(CO)_5$		$Fe_2(CO)_9$		$C_4H_6Fe(CO)_3$		$C_6H_8Fe(CO)_3$		$C_8H_8Fe(CO)_3$		assignment (final orbital)
E	T	E	T	E	T	E	T	E	T	
					L_3					
709.9	5.8	709.9	5.6	709.9	4.9	710.0	4.5	709.8	4.8	Fe 3d
711.8[a]	3.9	712.1[a]	3.4	711.7[a]	3.1	711.6[a]	2.9	711.6[a]	3.0	π^*(CO)
714.5	1.2	714.1	1.4							π^*(CO)
715.7[b]		715.5[c]		714.8[b]		714.46[b]		714.6[d]		IP
					L_2					
722.5	5.6	722.5	5.5	722.7	4.7	722.5	4.5	722.3	4.7	Fe 3d
742.2	3.9	724.6	3.4	724.2	3.2	724.3	2.7	724.2	2.9	π^*(CO)
728.1		728.0		727.4		727.0		727.1		IP[e]

[a] Calibration relative to CO_2 (O 1s → π^*: 535.4 eV): ΔE = 176.4 (3), 176.7 (2), and 176.3 (2) eV for $Fe(CO)_5$, $Fe_2(CO)_9$, and $C_8H_8Fe(CO)_3$. Calibration relative to SF_6 (F 1s → a_{1g}; 688.27 eV): ΔE = 23.33 (2) eV for $C_4H_6Fe(CO)_3$; to the O 1s → π^*(CO) of the same species ΔE = 177.9 (3) eV for c-$C_6H_8Fe(CO)_3$. [b] IP from XPS.[21] [c] IP assumed the same as for $Fe(CO)_5$. [d] IP estimated from values for the other $RFe(CO)_3$ species. [e] Derived from the L_3 IP by addition of the separation of the main L_3 and L_2 excitation peaks.

Table VII. Energies (E, ±0.2 eV), Term Values (T, eV), and Proposed Assignments for Features in the Fe 2p Spectra of $CpFeCpCH{=}CH_2$, $FeCp_2$, and $CpFeCpC_4H_9$

$CpFeCpC_2H_3$		$FeCp_2$		$CpFeCpC_4H_9$		
E	T	E	T	E	T	assignment (final orbital)
			L_3			
709.1[a]	3.9	708.9[a,b]	4.1	708.9[a]	4.1	$4e_{1g}$(-like), Fe 3d
711.7	1.3	711.5	1.5	711.3	1.7	$3e_{2u}$(-like), Cp π^*
713.0[c]		713.50[d]		713.0[c]		IP
			L_2			
721.4	3.9	721.2	4.2	721.2	3.9	$4e_{1g}$(-like), Fe 3d
724.2	1.1	723.9	1.5	723.8	1.5	$3e_{2u}$(-like), Cp π^*
725.3		725.4		725.3		IP[e]

[a] Calibration relative to CO_2 (O 1s → π^*: 535.4 eV): ΔE = 173.7 (3), 173.5 (4), and 173.5 (2) eV for $CpFeCpCH{=}CH_2$, $FeCp_2$, and $CpFeCpC_4H_9$, respectively. [b] Note these values are 0.6 eV higher than those reported previously[16] owing to an accurate recalibration. [c] IPs estimated from that of $Fe(Cp)_2$.[21] [d] IP from XPS.[21] [e] Derived from the L_3 IP by addition of the separation of the main L_3 and L_2 excitation peaks.

538 eV. This is much weaker than in the spectrum of free CO, as expected in bulky molecules due to greater valence–Rydberg mixing associated with the increased density of valence MOs. Because the oxygen atoms are at the periphery of these molecules, one might expect Rydberg transitions to be less "quenched" than at the C 1s edge. This factor is counterbalanced by the reduced size of the O 1s core orbital. The outcome seems to be a small absolute intensity but less change in Rydberg intensity from free CO at the O 1s than at the C 1s edge. Overall, the O 1s spectra of all of the complexes are very similar, not only in energy but also in relative intensity, signifying that they possess essentially the same origin. This is consistent with localization of the core excitation and very little modification of the virtual orbitals of the $Fe(CO)_3$ fragment with other changes in the molecule.

3. Fe 2p Spectra. The Fe 2p spectra of all eight species are compared in Figure 9. The energies, term values, and proposed assignments for the spectral features are listed in Tables VI and VII. As noted earlier,[16] the shape of metal 2p spectra correlates closely with the type of ligands in a complex. Among these species, the Fe 2p spectra of $Fe(CO)_5$ and $Fe_2(CO)_9$ are similar but quite distinct from those of ferrocene and substituted ferrocenes which, in turn, are distinct from the Fe 2p spectra of the $RFe(CO)_3$ species, whose spectra are in certain ways intermediate between those of the carbonyls and metallocenes. The Fe 2p spectra of $Fe(CO)_5$ and $Fe_2(CO)_9$ exhibit two features, with the lower energy band having only one-third to one-half of the intensity of the more intense, higher energy band. This pattern occurs at both the L_3 and L_2 edges. The close similarity of the shape of the L_3 and L_2 features is characteristic of the metal 2p spectra of all near-covalent complexes.[16] This is in distinct contrast to the spectra of

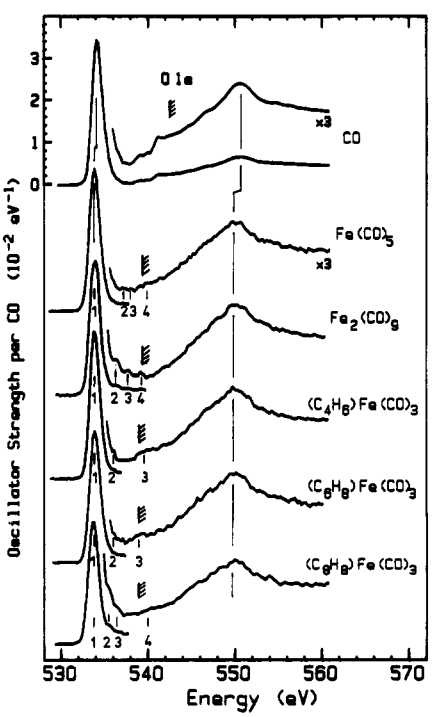

Figure 8. O 1s oscillator strength spectra of CO and the five CO-containing organoiron species derived from ISEELS spectra recorded under the conditions described in Figure 1. Each spectrum is presented in two parts, with the higher energy component amplified 3-fold.

ionic complexes and the predictions of crystal field calculations, where there are major differences between the shapes of the L_3 and L_2 components.[28]

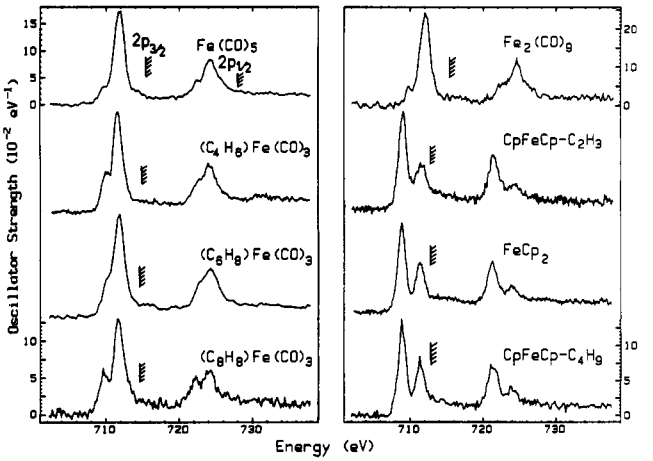

Figure 9. Fe 2p oscillator strength spectra of the eight organoiron complexes, derived from ISEELS spectra recorded under the conditions described in Figure 1. The hatched lines indicate the location of the Fe L_3 ($2p_{3/2}$) ionization potentials as measured by XPS[21] or estimated from similar species.

The apparently strong "ligand sensitivity" of metal 2p spectra has been noted previously, and a simple MO-based explanation has been proposed.[16] This model proposes that the shape of transition-metal 2p excitation spectra is closely related to the type of metal–ligand bonding and that this is a more important factor than the d-electron count or molecular symmetry, which are traditionally used to explain the electronic structure and spectra of organometallic complexes. In contrast to this qualitative MO model, de Groot et al.[28] have emphasized atomic multiplet effects and the importance of crystal field strength as determinants of metal 2p spectral shapes. Since the crystal field strength (as expressed by the $10Dq$ parameter of octahedral fields, for example) is closely related to the charge or dipole character of the ligands, the MO and crystal field models are not necessarily mutually incompatible. The challenge is to devise ways of using comparisons between calculation and experimental spectral recorded at modest resolution to distinguish the relative importance of multiplet, crystal field, and MO concepts in determining the metal 2p spectra of covalent complexes. As a step toward this goal, we have compared the experimental spectra of $Fe(CO)_5$ and $Fe_2(CO)_9$ with EHMO calculations and with the results of atomic multiplet calculations taken from the literature.[28]

The Fe 2p spectra of $Fe(CO)_5$ and $Fe_2(CO)_9$ are presented on an expanded scale in Figure 10, in comparison to the spectrum of Fe^{2+} (d^6) in an O_h field with $10Dq$ = 1.2, calculated by the atomic multiplet theory,[28] and to simulations derived from EHMO calculations of these carbonyl complexes. The atomic-multiplet-based predicted spectrum was smoothed slightly from the literature presentation to account for the experimental resolution. The EHMO-based simulated Fe 2p spectra were generated as for the C 1s simulated spectra except that c^2(Co3d) determined the intensity (peak area). The peak widths in the $Fe(CO)_5$ EHMO-based simulation were 0.7 eV except for the peak at 716 eV for which a 4-eV FWHM line width was assumed. The peak widths in the $Fe_2(CO)_9$ EHMO-based simulation were 1.0 eV except for the 716-eV peak where a width of 2.0 eV was used. The atomic multiplet

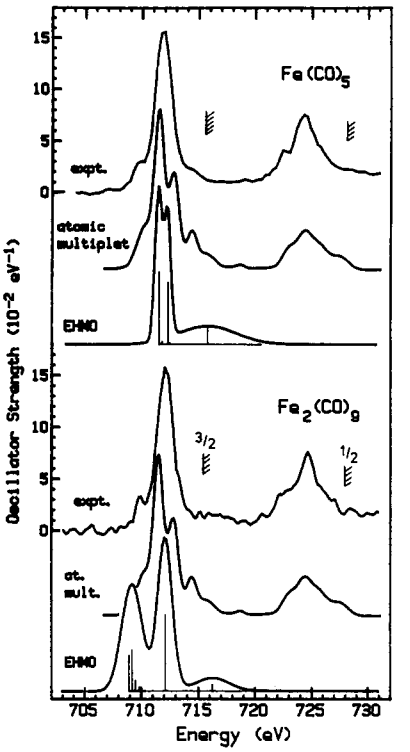

Figure 10. Comparison of the experimental Fe 2p spectra of $Fe(CO)_5$ and $Fe_2(CO)_9$ with EHMO spectral simulations of these species and the atomic multiplet calculation for Fe^{2+} (d^6) in an O_h field with $10Dq$ = 1.2.[28] In the EHMO simulation, the relative intensities are established from $\sum c^2$(Co3d) and the individual line widths are 0.7 eV (4 eV for the 715-eV peak) for $Fe(CO)_5$ and 1.0 (2 eV for the 715-eV peak) for $Fe_2(CO)_9$. The main line of the EHMO calculation is aligned with the main peak of the experimental spectrum. The digitized atomic multiplet spectrum[28] has been smoothed in order to better match our experimental resolution and shifted by 1.6 eV to align the main L_3 peak. For both predicted spectra, the intensity scale was calibrated from the area of the experimental spectrum between 707 and 716 eV.

theory clearly provides a superior representation of the spectrum even though the symmetry and ionic charge are not correct.

According to the EHMO results, almost all of the low-lying virtual orbitals of the iron carbonyls have a dominant π^*(CO) character with varying admixtures of Fe 3d. It is the latter which is associated with the Fe 2p spectra. A low-intensity band is observed between 709 and 710 eV in the spectra of both species. The EHMO calculation does not predict any feature in this region for $Fe(CO)_5$ and provides only a poor match for $Fe_2(CO)_9$. In contrast, the atomic multiplet calculation reproduces almost all of the structure in the experimental spectra, both in position and relative intensity. The most intense peak at 712 eV in each species is assigned to Fe 2p excitation to the Fe 3d component of the main density of π^*(CO) MOs. According to the EHMO results, the intense 712-eV peak arises mostly from excitations to a small number of π^*(CO)-type MOs (two in $Fe(CO)_5$ and one in $Fe_2(CO)_9$). There is rather serious disagreement in the lowest energy region for $Fe_2(CO)_9$. EHMO suggests there should be quite strong excitations to a number of orbitals, the lowest energy of which is of σ^*(Fe–Fe) character. However, while the $Fe_2(CO)_9$ spectrum does have intensity in this region, so does $Fe(CO)_5$, but EHMO does not predict this.

Metal carbonyls have a strong preference for adopting an 18-e^- configuration at the metal in order to achieve coordinative saturation. CO ligands also favor the formation of M–M bonds[12] and metal clusters, due to their small size and the fact that their bonds to metals are co-

(28) de Groot, F. M. F.; Fuggle, J. C.; Thole, B. T.; Sawatzky, G. A. *Phys. Rev. B* **1990**, *42*, 5459. de Groot, F. M. F.; Fuggle, J. C.; Thole, B. T.; Sawatzky, G. A. *Phys. Rev. B* **1990**, *41*, 928. de Groot, F. M. F.; Grioni, M.; Fuggle, J. C.; Ghijsen, J.; Sawatzky, G. A.; Petersen, H. *Phys. Rev. B* **1989**, *40*, 5715.

valent rather than ionic, which leaves the metal atom in an environment perhaps similar to that of the bulk metal. Cotton[18] interprets $Fe_2(CO)_9$ as having a single Fe–Fe bond. This is consistent with the short Fe–Fe distance of 2.523 Å. From the weak bond concept[29] and MO considerations, a low-lying σ^*(Fe–Fe) MO of large Fe 3d character is expected in $Fe_2(CO)_9$. Transitions to such an orbital should appear as low-lying features in the Fe 2p (and Fe 3p) spectra. However, the experimental Fe 2p spectra do not support these concepts. It seems that either the Fe $2p \rightarrow \sigma^*$(Fe–Fe) transition is too weak to be detected or the σ^*(Fe–Fe) character is distributed over such a large number of MOs that there is very little difference from the spectrum of mononuclear metal complexes.

The crystal field/atomic multiplet approach to the 2p X-ray absorption of 3d transition-metal compounds[28] predicts that such spectra should have a very complex multiplet-line structure, typically consisting of many hundreds of lines for 3d elements such as Fe, which are in the middle of the period and have a large d count. A series of X-ray absorption metal 2p spectra of ionic complexes in the solid state[28,30] at systematically increased resolution have been reported recently. With each improvement in resolution, additional spectral detail is revealed, supporting the belief that metal 2p spectra are very complex. If this atomic-like model is relevant to covalent organoiron complexes, explaining the detailed origin of metal 2p spectra will be beyond the capabilities of EHMO. de Groot et al.[28] and Chen and Sette[30] have presented examples of the very complex, many-line spectra that appear to be characteristic of metal 2p core excitation. The multiplet/crystal field theory of de Groot et al.[28] seems to be very successful in predicting the spectra of ionic 3d complexes as well as complexes with ligands such as cyanide which generate large crystal fields.[31] The degree of relevance of this approach to the spectroscopy of more covalent, weak crystal field transition-metal compounds remains to be determined. Certainly inclusion of MO considerations, i.e., full ligand field theory, has been found to be important in obtaining a proper understanding of the electronic structure and chemical properties of 3d transition-metal complexes. It is possible, however, that the short-range, spatially localized character of core excitation could mean that the 3d density in the region of the compact 2p core orbital is adequately described by a theory which only considers the effective charge that the ligands present to the small-R region of the Fe 3d orbitals. In that case, crystal field theory could be adequate.

The Fe 2p spectra of the three $RFe(CO)_3$ species are similar to each other and more similar to the iron carbonyls than to the ferrocenes, as found at the C 1s edge. Parallel to the carbonyls, we assign the most intense peak to Fe 2p excitations to the Fe 3d component of the π^*(CO) MOs. The greatest difference from the Fe 2p spectra of the carbonyls is the greater intensity and higher energy of the first band around 710 eV in the spectrum. This band also varies considerably among the three $RFe(CO)_3$ species. It is best resolved in $C_8H_8Fe(CO)_3$ and least well-resolved in $C_6H_8Fe(CO)_3$. Clearly the first feature is more strongly associated with the π-bonded R group than the $Fe(CO)_3$ fragment. The Fe 2p spectra of the ferrocenes have their strongest transition at 709 eV, very close to the energy of the first peak in the Fe 2p spectra of the $RFe(CO)_3$ complexes. The η^4 bond of dienes is similar to the η^5 bond of a Cp. Thus, one might expect that the additional intensity in the 710-eV peak observed in the $RFe(CO)_3$ complexes relative to the pure iron carbonyls has an origin similar to that for the main peak in the Fe 2p spectra of the ferrocenes, namely, Fe 2p excitations to an orbital of mainly Fe 3d character but with admixture of π(C=C). In addition, the three $RFe(CO)_3$ complexes show small variations in the shape of the 710-eV peak which are similar to the variations in the shapes of the lowest energy peak in the C 1s spectra of the same species. This suggests that the π^*(C=C) and $4e_{1g}$-like orbitals, which are believed to be relevant in the C 1s spectrum, are also the final orbitals in the lowest energy Fe 2p excitations. However, it is the Fe 3d component of these orbitals rather than the C 2p component which determines the relative intensity. Higher resolution ISEELS or X-ray absorption spectra would be very useful to further investigate the parallels between the C 1s and Fe 2p spectra.

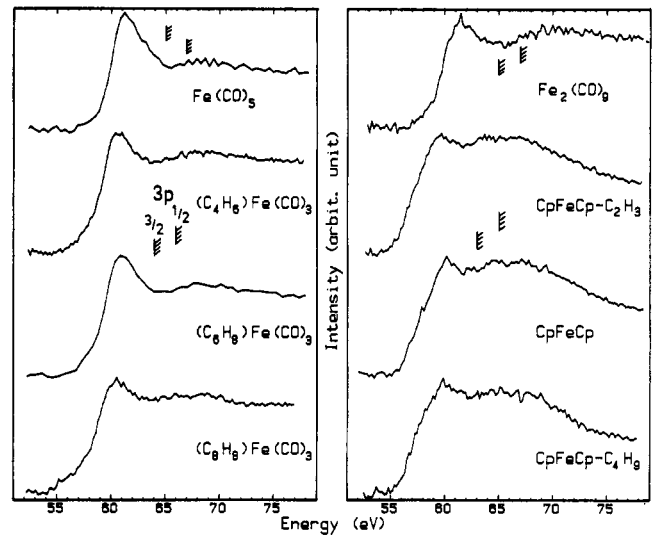

Figure 11. Fe 3p energy loss spectra of the eight organoiron complexes. A smooth curve extrapolated from the valence continuum background has been subtracted from each spectrum. The *S:B* at the Fe 3p edge was typically 1:10. The hatched lines indicate the $3p_{3/2}$ and $3p_{1/2}$ IPs estimated from the atomic 3p IP[33] and the chemical shifts of the $2p_{3/2}$ IPs.

The dramatic change between the Fe 2p spectra of the ferrocenes and the iron carbonyl complexes well-illustrates the strong dependence of the Fe 2p spectra on ligand type. Again, the spectra of the three ferrocene complexes are quite similar, indicating that alkyl or vinyl substitution has very little influence on the Fe 2p excitation of ferrocene. This could be a consequence of the large distance between the Cp substituents and the Fe 3d orbitals directly involved in the Fe 2p excitation. The most intense peak at 709 eV is ascribed to Fe $2p \rightarrow 4e_{1g}$-like transitions since simple MO concepts and EHMO calculations[7,15,16] indicate these orbitals have a large Fe 3d contribution. The less intense peak around 711 eV is attributed to Fe $2p \rightarrow 3e_{2u}$-like excitations. The $3e_{2u}$ MO is localized largely on the Cp rings of the molecule. Thus, this excitation has metal-to-ligand charge-transfer character.[16] While the reduced symmetry of the substituted ferrocenes should split the degeneracy of both the $4e_{1g}$-like and $3e_{2u}$-like MOs, there is no clear indication of this effect. A pseudodegenerate character of these virtual MOs is suggested by valence excitation spectroscopy of ring-substituted ferrocenes.[32] The latter work showed that substituted fer-

(29) Ishii, I.; Mclaren, R.; Hitchcock, A. P.; Robin, M. B. *J. Chem. Phys.* **1987**, *87*, 4344.
(30) Chen, C. T.; Sette, F. *Phys. Scr.* **1990**, *T31*, 119.
(31) Cramer, S. P.; et al. Unpublished work.
(32) Dowben, P. A.; Driscoll, D. C.; Tate, R. S.; Boag, N. M. *Organometallics* **1988**, *7*, 305 and references therein.

rocenes have similar electronic structures to that of $Fe(Cp)_2$ and that substituents cause very small energy shifts but no changes in orbital ordering.

4. Fe 3p Spectra. The Fe 3p spectra of the eight complexes are presented in Figure 11 on a common energy scale. A smooth background extrapolated from the underlying valence-shell continuum has been subtracted. No attempt was made to convert these spectra to oscillator strength scales or to derive a detailed assignment. Broadly, the 3p spectra are characterized by two features. The peak at 60 eV occurs below the 3p IP, which is estimated to be about 66 eV.[33] This peak likely arises from Fe 3p excitations to the Fe 3d component of the lower energy MOs responsible for the Fe 2p structure. It is possible the individual transitions making up this feature have nonsymmetric Fano line shapes. Evidence for this has been presented in studies of the momentum transfer dependence of the Ni 3p edge of solid Ni,[34] and the calculations of van der Laan[35] predict significant interaction between the 3p excited states and the underlying 3d continuum, the phenomenon responsible for Fano line shapes. A broad band around 68 eV is also a common feature of all eight spectra. Both of these spectral features likely comprise a number of unresolved $3p_{3/2}$ and $3p_{1/2}$ components.

As noted earlier,[16] the shapes of the 3p spectra appear to track those of the Fe 2p spectra, with the same systematic relationship to types of ligand. In particular, the 60-eV peak of the carbonyl complexes has an abrupt edge with a low-energy shoulder, while the ferrocene complexes have a more rounded peak with distinct evidence of a shoulder which could be the relatively intense low-lying Fe $3p_{3/2} \rightarrow 4e_{1g}$ peak. The shift by around 2 eV to lower energy in the Fe 3p → 3d structure in $Fe(Cp)_2$ and derivatives relative to that in the carbonyl complexes is associated with a lower Fe 3p ionization energy, based on the 2-eV chemical shift between the Fe $2p_{3/2}$ IP of ferrocene and $Fe(CO)_5$.[20]

Recently, van der Laan[35] has predicted the 3p absorption spectra of 3d transition-metal compounds using the atomic multiplet and crystal field description developed by de Groot et al.[28] These calculations predict that there should be a multiple-line structure but that the visibility of the individual lines is very dependent on the experimental resolution and natural line width as well as the interplay of the exchange, spin–orbit, and crystal field interactions for a given complex. This is well-illustrated by the high-resolution metal 3p spectra of the transition-metal atoms[36] which show clearly resolved multiplet structure. The crystal field calculations show that it is the overlap of the two spin–orbit components, combined with resolution limitations, which causes the M_{23} spectrum to have only one strong line, whereas the L_{23} spectrum has at least two strong lines. Interestingly, the van der Laan[35] calculations do predict a higher energy peak in the region of the broad, 67-eV continuum feature. However, it is most prominent in calculations carried out with large crystal field, whereas experimentally the 67-eV peak is strongest in the ferrocene complexes, which should have a weaker crystal field than the carbonyl complexes.

As with the Fe 2p spectrum, comparison of the Fe 3p spectra of $Fe(CO)_5$ and $Fe_2(CO)_9$ could potentially provide evidence for excitations to σ^*(Fe–Fe) orbitals. This comparison suggests there is additional intensity around 58 eV in the $Fe_2(CO)_9$ spectrum relative to that of $Fe(CO)_5$. This could be evidenced for Fe $3p_{3/2} \rightarrow \sigma^*$(Fe–Fe) transitions in $Fe_2(CO)_9$. However, this difference is rather sensitive to the details of the background subtraction, and there are similar low-energy shoulders in some of the other complexes containing only a single Fe atom. More convincing evidence for a M np → σ^*(M–M) feature has recently been observed in the Co 2p and Co 3p spectra of complexes containing 3 Co atoms, $RC[Co(CO)_3]_3$.[37]

V. Summary

The C 1s, O 1s, Fe 2p, and Fe 3p spectra of eight organoiron complexes have been recorded under dipole conditions. They have been converted to oscillator strengths and assigned tentatively on the basis of spectral comparisons, EHMO calculations, spectral simulations, and comparison with previous studies of related organometallic species and the free ligand molecules. While the EHMO results do not fully reproduce all aspects of the experimental spectra, they certainly are useful for providing insights into the effect of the core hole and for giving more information than is available from a solely experimentally-based assignment procedure.

Each edge in the series shows a certain pattern and reveals complementary, spatially localized, symmetry-selected information about the unoccupied electronic structure of these complexes. The C 1s spectra are the most sensitive to minor substituent effects, as expected since the substituents in all cases contain carbon and many of these carbon atoms are directly involved in the ligand–metal bonding. All of the O 1s spectra are quite similar, indicative of a strong chromophoric character to the $Fe(CO)_3$ fragment. The Fe 2p spectra are quite sensitive to the type of ligand but insensitive to chemical substitution at remote locations on the ligands. The Fe 3p spectra are the least informative. As in previous studies of other metal–metal binuclear complexes ($Mn_2(CO)_{10}$[3] and $Co_2(CO)_8$[15]), compelling evidence for inner-shell excitations to a σ^*(Fe–Fe) MO in $Fe_2(CO)_9$ was not found. Investigations of complexes with a greater number of metal–metal bonds[37] and/or compounds with multiple metal–metal bonds are expected to be more fruitful in this regard.

Acknowledgment. This work is supported by NSERC (Canada) and a NATO scientific exchange grant. We are grateful to Dr. T. Tyliszczak for much technique assistance in optimizing the spectrometer, designing and constructioning the electronics, and building an improved collision cell heater.

OM9107552

(33) Shirley, D. A.; Martin, R. L.; Kowalczyk, S. P.; McFeeley, F. R.; Ley, L. *Phys. Rev. B* **1977**, *15*, 544.
(34) Dietz, R. E.; McRae, E. G.; Taft, Y.; Caldwell, C. W. *Phys. Rev. Lett.* **1974**, *33*, 1372.
(35) van der Laan, G. *J. Phys. Condensed Matter* **1991**, *3*, 7443.
(36) Meyer, M.; Prescher, Th.; Von Raven, E.; Richter, M.; Schmidt, E.; Sonntag, B.; Wetzel, H. E. *Z. Phys. D.* **1986**, *2*, 347.
(37) Johnson, A. L.; Walter, W. K.; Perez-Jigato, M.; King, D. A.; Norman, D.; Rühl, E.; Schmale, C.; Baumgärtel, H.; McGlinchey, M. J.; Hitchcock, A. P. In preparation.